

# Haptoglobin Interacts with Apolipoprotein E and Beta-Amyloid and Influences Their Crosstalk

Maria Stefania Spagnuolo,<sup>†</sup> Bernardetta Maresca,<sup>‡</sup> Valeria La Marca,<sup>‡</sup> Albino Carrizzo,<sup>§</sup> Carlo Veronesi,<sup>||</sup> Chiara Cupidi,<sup>⊥</sup> Tommaso Piccoli,<sup>#</sup> Raffaele Giovanni Maletta,<sup>⊥</sup> Amalia Cecilia Bruni,<sup>⊥</sup> Paolo Abrescia,<sup>‡</sup> and Luisa Cigliano<sup>\*;‡</sup>

<sup>†</sup>ISPAAM, Consiglio Nazionale delle Ricerche, via Argine 1085, 80147 Napoli, Italia

<sup>‡</sup>Dipartimento di Biologia, Università di Napoli Federico II, via Mezzocannone 8, 80134 Napoli, Italia

<sup>§</sup>I.R.C.C.S. Neuromed, Unità di Fisiopatologia Vascolare, via Atinense 18, 86077 Pozzilli (IS), Italia

<sup>||</sup>Dipartimento di Scienze Biomediche e Chirurgico Specialistiche, Sezione di Fisiologia Umana, Università di Ferrara, via Fossato di Mortara 19, 44100 Ferrara, Italia

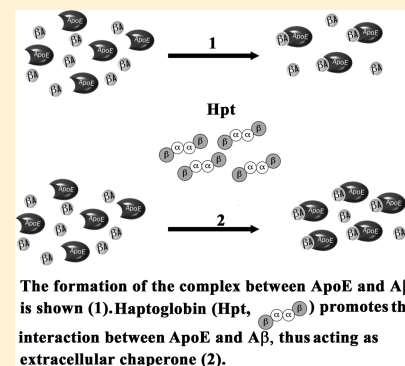
<sup>⊥</sup>Centro Regionale di Neurogenetica, via Perugini, ASP Catanzaro, 88046 Lamezia Terme (CZ), Italia

<sup>#</sup>Dipartimento di Biomedicina Sperimentale e Neuroscienze Cliniche (BioNeC), Università di Palermo, via del Vespro, 90127 Palermo, Italia

## Supporting Information

**ABSTRACT:** Beta-amyloid accumulation in brain is a driving force for Alzheimer's disease pathogenesis. Apolipoprotein E (ApoE) represents a critical player in beta-amyloid homeostasis, but its role in disease progression is controversial. We previously reported that the acute-phase protein haptoglobin binds ApoE and impairs its function in cholesterol homeostasis. The major aims of this study were to characterize the binding of haptoglobin to beta-amyloid, and to evaluate whether haptoglobin affects ApoE binding to beta-amyloid. Haptoglobin is here reported to form a complex with beta-amyloid as shown by immunoblotting experiments with purified proteins, or by its immunoprecipitation in brain tissues from patients with Alzheimer's disease. The interaction between ApoE and beta-amyloid was previously shown to be crucial for limiting beta-amyloid neurotoxicity and for promoting its clearance. We demonstrate that haptoglobin, rather than impairing ApoE binding to beta-amyloid, promotes to a different extent the formation of the complex between beta-amyloid and ApoE2 or ApoE3 or ApoE4. Our data suggest that haptoglobin and ApoE functions in brain should be evaluated taking into account their mutual interaction with beta-amyloid. Hence, the risk of developing Alzheimer's disease might not only be linked to the different ApoE isoforms, but also rely on the level of critical ligands, such as haptoglobin.

**KEYWORDS:** Beta-amyloid, haptoglobin, apolipoprotein E, ApoE/A $\beta$  complex, Alzheimer's disease, human brain tissue



Alzheimer's disease (AD) is a devastating neurodegenerative disease, characterized by progressive loss of memory and cognitive functions. Pathological hallmark of AD are extracellular accumulation of beta amyloid (A $\beta$ ), intracellular accumulation of tau, neuronal death, brain atrophy, and inflammation.<sup>1,2</sup> In vivo, apolipoprotein E (ApoE) is associated with amyloid senile plaques, and in vitro lipid-bound or free ApoE can form stable complexes with A $\beta$  peptides.<sup>3–5</sup> ApoE is the major component of brain HDL-like lipoproteins and is implicated in the regulation of cholesterol and A $\beta$  metabolism.<sup>6</sup> In humans, ApoE is a polymorphic protein with three common isoforms, ApoE2, ApoE3, and ApoE4, with single amino acid substitutions resulting in crucial functional differences.<sup>2,7</sup> ApoE4 is associated with increased risk of AD.<sup>6,8</sup> Although there is evidence that ApoE isoforms can differently influence A $\beta$  aggregate formation and toxic effects,<sup>6</sup> ApoE involvement in AD pathogenesis remains controversial.

A research strategy might be to focus on factors that modulate ApoE function. In this frame, we previously reported that haptoglobin (Hpt), an acute-phase protein of inflammation, binds ApoE and influences key roles of this apolipoprotein in cholesterol homeostasis.<sup>9</sup> Hpt is synthesized primarily by hepatocytes, and to a lesser extent in other tissues including lung, skin, and brain.<sup>10,11</sup> Hpt is best known for its role in hemoglobin (Hb) binding and transport to the liver.<sup>12</sup> Although Hpt was first suggested as a marker of blood-brain barrier dysfunction,<sup>13</sup> recent studies pointed out that oligodendrocytes and astrocytes produce it in response to different stress stimuli.<sup>14–16</sup> Interestingly, an increased level of Hpt was found in cerebrospinal fluid (CSF) from patients with

Received: May 8, 2014

Revised: July 24, 2014

Published: July 24, 2014

AD,<sup>17</sup> or other neurodegenerative diseases such as Parkinson's and Huntington's disease.<sup>18,19</sup> Like other extracellular chaperones, such as clusterin and  $\alpha 2$ -macroglobulin, Hpt colocalizes with amyloid plaques in AD<sup>20–22</sup> and inhibits  $A\beta$  fibril formation in vitro.<sup>22</sup> Recently, Hpt was reported to be increasingly oxidized in AD patients, and in vitro oxidation of this protein was shown to affect its ability to prevent formation of amyloid aggregates.<sup>23</sup>

Since the role of Hpt in AD pathogenesis has not been fully investigated to date, the binding of Hpt to ApoE conceals an intriguing scenario in which Hpt might significantly influence the function of both ApoE and  $A\beta$ .

In this study, the interaction between Hpt and  $A\beta$  was characterized, and the effect of Hpt on the ability of ApoE to bind  $A\beta$  was evaluated. We report here, for the first time, that Hpt binds both  $A\beta_{1-40}$  and  $A\beta_{1-42}$ , and an SDS-stable complex between Hpt and  $A\beta$  is produced in experimental conditions similar to those described for the production of the ApoE/ $A\beta$  stable complex.<sup>24</sup> ApoE and  $A\beta$  co-immunoprecipitate with Hpt in human brain tissues from AD patients. Moreover, we show that Hpt does not impair the binding of ApoE to  $A\beta$ , but facilitates the formation of the ApoE/ $A\beta$  stable complex, also when  $A\beta$  naturally produced by the 7PA2 line, a well characterized AD cell model,<sup>25–27</sup> was used. In particular, Hpt effect was more pronounced just in the presence of ApoE4, that causally contributes to AD pathogenesis.

## RESULTS

**Binding of Hpt to  $A\beta$ .** Hpt 2-1 was previously shown to interact with prefibrillar species of  $A\beta$ .<sup>22</sup> As the three human Hpt phenotypes (namely, Hpt 1-1, 2-2, and 2-1) present different prevalence in several diseases,<sup>28</sup> we compared them for the ability of binding  $A\beta_{1-40}$  or  $A\beta_{1-42}$ . As shown in Figure 1, the amount of Hpt bound to  $A\beta$  increased with the concentration of Hpt in the incubation medium. By comparing the  $K_d$  of each Hpt phenotype for  $A\beta_{1-40}$  (Figure 1, panel A) and for  $A\beta_{1-42}$  (Figure 1, panel B), we found that the three phenotypes did not differ for the binding to  $A\beta$ , and that each Hpt phenotype binds  $A\beta_{1-40}$  and  $A\beta_{1-42}$  with similar efficiency ( $K_d$  Hpt 1-1,  $A\beta_{1-40}$   $0.337 \pm 0.050 \mu\text{M}$ ,  $A\beta_{1-42}$   $0.326 \pm 0.074 \mu\text{M}$ ;  $K_d$  Hpt 2-2,  $A\beta_{1-40}$   $0.305 \pm 0.097 \mu\text{M}$ ,  $A\beta_{1-42}$   $0.338 \pm 0.119 \mu\text{M}$ ;  $K_d$  Hpt 2-1,  $A\beta_{1-40}$   $0.241 \pm 0.075 \mu\text{M}$ ,  $A\beta_{1-42}$   $0.342 \pm 0.112 \mu\text{M}$ ).

Further, as the Hpt ability to inhibit amyloid fibril formation was found reduced when this protein is complexed with Hb,<sup>22</sup> we investigated whether the binding of Hpt to Hb is impaired in the presence of  $A\beta$ . Hb-coated wells ( $0.125 \mu\text{M}$ ) were incubated with mixtures containing  $0.3 \mu\text{M}$  Hpt and different amounts of  $A\beta_{1-40}$  or  $A\beta_{1-42}$  ( $1\text{--}10 \mu\text{M}$ , corresponding to 8–80 molar excess over the concentration of Hb immobilized into the wells). As shown in Figure S1 in the Supporting Information, Hpt binding to Hb decreased as the amount of  $A\beta$  increased, thus suggesting that a competition between Hb and  $A\beta$  for binding Hpt does exist. The competitive inhibition of  $A\beta_{1-40}$  on Hpt 2-2 binding to Hb was found to be higher than those of Hpt 2-1 or Hpt 1-1 ( $p < 0.01$ ), in agreement with the lower binding affinity of the phenotype Hpt 2-2 to Hb.<sup>29</sup>

### SDS-Stable Complex Formation between Hpt and $A\beta$ .

To further characterize the interaction between Hpt and  $A\beta$ ,  $A\beta_{1-40}$  ( $220 \mu\text{M}$ ) was incubated (6 h,  $37^\circ\text{C}$ ) with  $3 \mu\text{M}$  Hpt. Samples were analyzed by electrophoresis on 4–20% polyacrylamide gel, under denaturing but nonreducing conditions (4–20% PAGE-D), followed by Coomassie staining

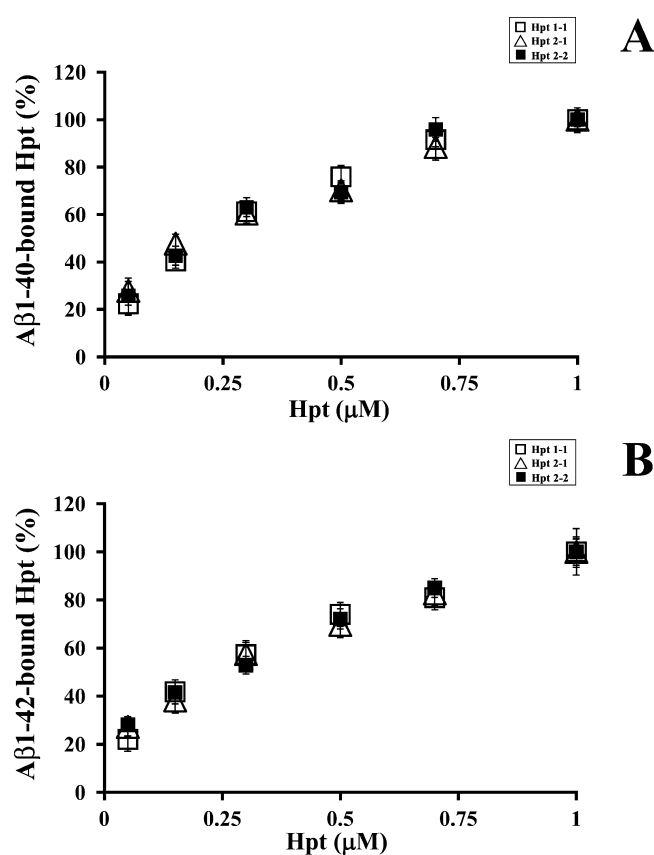


**Figure 1.** Hpt binding to  $A\beta$ . Aliquots of  $0.45 \mu\text{M}$   $A\beta_{1-40}$  (A) or  $A\beta_{1-42}$  (B) were loaded into the wells of a microtiter plate and incubated with different concentrations ( $0.05\text{--}1 \mu\text{M}$ ) of Hpt 1-1 (open squares), Hpt 2-1 (open triangles), or Hpt 2-2 (solid squares). Hpt bound to  $A\beta$  was detected by using rabbit anti-Hpt and GAR-HRP IgGs, measured as absorbance at 492 nm, and reported as percentage of the value obtained with  $1 \mu\text{M}$  protein (assumed as 100% of Hpt binding to  $A\beta$ ). Samples were processed in triplicate. Data were expressed as mean  $\pm$  SEM versus micromolar concentration.

or immunostaining. Under the nonreducing conditions utilized,  $A\beta$  migrated as a 4.3 kDa band, while Hpt 1-1 as an 86 kDa band (Figure 2, panel A, Coomassie staining, lanes 2 and 3, respectively). In the mixture containing both Hpt 1-1 and  $A\beta_{1-40}$ , the Hpt band was missing, and a protein band of about 97 kDa was detected (Figure 2, panel A, Coomassie staining, lane 4), thus suggesting the presence of a complex between  $A\beta$  and Hpt. In fact, when the mixtures were analyzed by Western Blot, both anti- $A\beta$  IgG and anti-Hpt IgG reacted to the 97 kDa band (Figure 2, panel A, lane 3), thus confirming that Hpt can form an SDS-stable complex with  $A\beta_{1-40}$ , under experimental conditions similar to those used for the detection of the ApoE/ $A\beta$  complex.<sup>3,24</sup>

The Hpt/ $A\beta$  stable complex was also detectable when lower amounts of peptide and Hpt were used. As a matter of fact, we found a band reacting with both anti- $A\beta$  IgG and anti-Hpt IgG when  $A\beta_{1-42}$  or  $A\beta_{1-40}$  ( $10 \mu\text{M}$ ) was incubated with  $0.5$  or  $1.5 \mu\text{M}$  Hpt (Figure S2, panels A and B, respectively). Further, a protein band of about 97 kDa, reacting with both anti- $A\beta$  and anti-Hpt IgGs, was detected in pooled brain tissues (hippocampus and cortex) of AD patients (Figure S2, panel C).

The effect of time and Hpt concentration on the interaction between Hpt and  $A\beta$  was investigated by using the physiological concentrations of Hpt in plasma.<sup>12</sup>  $A\beta_{1-40}$  ( $220$

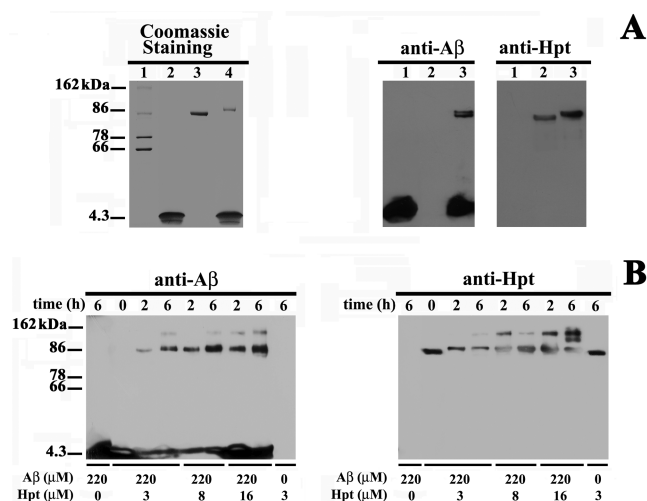


**Figure 2.** SDS-stable complex formation between Hpt and A $\beta$ . (A) Hpt (3  $\mu$ M) was incubated (6 h, 37  $^{\circ}$ C) in the absence or presence of A $\beta$ <sub>1-40</sub> (220  $\mu$ M). The samples were analyzed by 4–20% PAGE-D, followed by Coomassie staining or Western blotting. Coomassie staining: Lane 1, molecular weight markers (IgG, 162, kDa; Hpt 1-1, 86 kDa; Transferrin, 78 kDa; BSA, 66 kDa; A $\beta$ <sub>1-40</sub>, 4.3 kDa). Lane 2, A $\beta$ <sub>1-40</sub>. Lane 3, Hpt 1-1. Lane 4, mixture of Hpt 1-1 and A $\beta$ <sub>1-40</sub>. Western blotting: A $\beta$ <sub>1-40</sub> (lane 1), Hpt 1-1 (lane 2), mixture of Hpt 1-1 and A $\beta$ <sub>1-40</sub> (lane 3) probed with mouse anti-A $\beta$ -IgG 6E10 or with rabbit anti-Hpt IgG. (B) A $\beta$ <sub>1-40</sub> (220  $\mu$ M) was incubated with 3, 8, or 16  $\mu$ M Hpt (0, 2, or 6 h, 37  $^{\circ}$ C). Samples were analyzed by 4–20% PAGE-D and Western blotting. Immunodetection was carried out with mouse anti-A $\beta$  and GAM-HRP IgGs or by rabbit anti-Hpt and GAR-HRP IgGs. In each panel, a single representative of at least three independent experiments is shown.

$\mu$ M) was incubated with 3, 8, or 16  $\mu$ M Hpt for 2 or 6 h at 37  $^{\circ}$ C. A higher amount of the 97 kDa complex was found by increasing both Hpt concentration and time of incubation (Figure 2, panel B). In particular, when Hpt concentration in the reaction mixture was 8  $\mu$ M or 16  $\mu$ M, a further complex of about 155 kDa, reacting with both anti-A $\beta$  and anti-Hpt IgGs was found (Figure 2, panel B). In these conditions, a higher amount of A $\beta$  might be engaged in the SDS-stable complex with Hpt.

#### Competition between Hpt and A $\beta$ for Binding ApoE.

As both Hpt and ApoE interact with A $\beta$ ,<sup>3,22</sup> and Hpt also binds ApoE,<sup>9</sup> we investigated, by ELISA, whether a competition between Hpt and A $\beta$  for binding ApoE does exist. These experiments were carried out with liposome-embedded ApoE (Lipo-E) instead of free ApoE, as this apolipoprotein, in brain, is mostly associated with HDL-like particles.<sup>30–33</sup> A $\beta$ -coated wells were incubated with mixtures containing 0.01  $\mu$ M LipoE2, LipoE3, or LipoE4 and different concentrations of Hpt 1-1 (0–0.1  $\mu$ M). Hpt did not significantly reduce the binding of LipoE2, LipoE3, or LipoE4 to A $\beta$ <sub>1-42</sub> (Figure 3). Also, the binding of LipoE2 and LipoE4 to A $\beta$ <sub>1-40</sub> was not impaired in the presence of Hpt, at any concentration assayed (Figure 3, panels A and C), while even at the highest Hpt concentration used (presumed 10-fold excess over ApoE in the mixture) LipoE3 binding to A $\beta$ <sub>1-40</sub> was only reduced to 68% ( $p < 0.01$ ; Figure 3, panel B). These results suggest that Hpt does not interfere with the apolipoprotein binding to A $\beta$ , and that ApoE essentially retains the ability to bind A $\beta$  also when Hpt concentration increases, as occurs during inflammatory conditions.

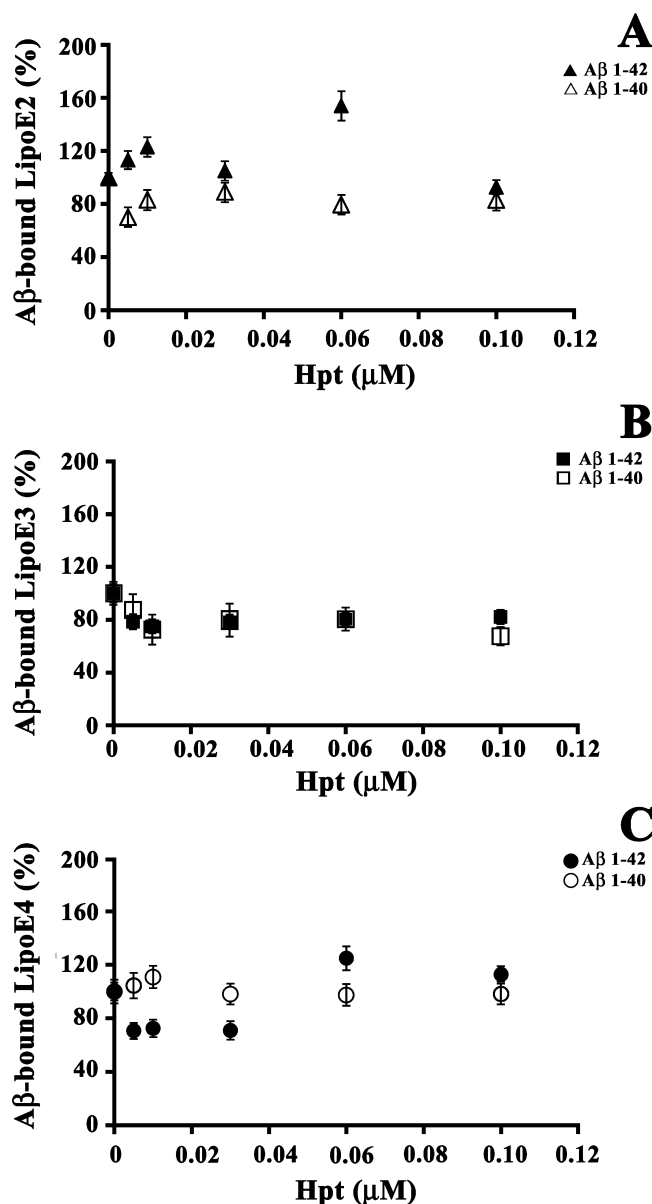


**Figure 3.** Competition between Hpt and A $\beta$  for binding ApoE. Aliquots of mixtures containing 0.01  $\mu$ M liposome-embedded ApoE (LipoE2, LipoE3, or LipoE4) and different concentrations (0.005–0.1  $\mu$ M) of Hpt 1-1 were loaded into A $\beta$ -coated wells. The amount of ApoE bound to A $\beta$  was detected by using goat anti-ApoE and RAG-HRP IgGs. Samples were analyzed in triplicate. Data are reported as percentage of the absorbance value obtained by incubation of ApoE alone (assumed as 100% of ApoE binding to A $\beta$ ) and expressed as mean  $\pm$  SEM. (A) Binding of Lipo E2 to A $\beta$ <sub>1-40</sub> (open triangles) or to A $\beta$ <sub>1-42</sub> (full triangles). (B) Binding of LipoE3 to A $\beta$ <sub>1-40</sub> (open squares) or to A $\beta$ <sub>1-42</sub> (full squares). (C) Binding of LipoE4 to A $\beta$ <sub>1-40</sub> (open circles) or to A $\beta$ <sub>1-42</sub> (full circles). In each panel, a single representative of at least three independent experiments is shown.

#### Immunoprecipitation of Hpt in Human Brain Homogenates or in CSF.

Post-mortem brain tissues (hippocampus and cortex) from two AD patients and one control subject were processed by electrophoresis and Western blotting, for detecting A $\beta$  and Hpt. Immunodetection with mouse antibody 6E10 (against A $\beta$  residues 1–16) revealed the presence of A $\beta$  monomers only in hippocampus and cortex from AD1 patient (Figure 4, panel A, anti-A $\beta$ , lanes 2, 3), while amyloid precursor

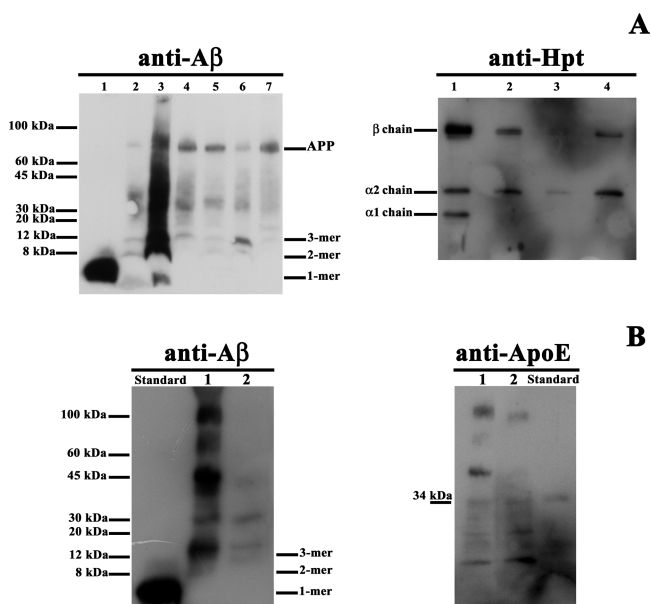


**Figure 4.** Analysis of post-mortem AD brain tissues. (A) Anti- $A\beta$ : Aliquots (50  $\mu\text{g}$ ) of hippocampus or cortex from brain of two AD patients (namely, 1 and 2) and one control subject were processed by 4–20% PAGE-D, and Western blotting. Immunodetection was carried out with mouse anti- $A\beta$ -IgG 6E10 and GAM-HRP IgG. Lane 1,  $A\beta_{1-42}$  standard (100 ng). Lane 2, hippocampus from AD patient 1. Lane 3, cortex from AD patient 1. Lane 4, hippocampus from AD patient 2. Lane 5, cortex from AD patient 2. Lane 6, hippocampus from control subject. Lane 7, cortex from control subject. Anti-Hpt: Pool of hippocampus and cortex from each AD patient and control subject were analyzed by 15% SDS PAGE, under reducing conditions, and Western blotting. Immunodetection was carried out with rabbit anti-Hpt IgG and GAR-HRP IgG. Lane 1, Hpt 2-1 standard (100 ng). Lanes 2–4, brain tissue from AD patient 1, AD patient 2, and control subject, respectively. (B) A pool of hippocampus and cortex from AD patients 1 and 2 and a pool of hippocampus and cortex from a control subject were immunoprecipitated with rabbit anti-Hpt IgG. Immunoprecipitates were processed by 4–20% PAGE-D and Western blotting. After blotting onto a PVDF membrane, the membrane was immunostained with mouse anti- $A\beta$  and GAM-HRP IgGs or with goat anti-ApoE and RAG-HRP IgGs. Anti- $A\beta$ : Standard,  $A\beta_{1-42}$  (100 ng). Lane 1, immunoprecipitate of AD tissues. Lane 2, immunoprecipitate of control tissues. Anti-ApoE: Lane 1, immunoprecipitate of AD tissues. Lane 2, immunoprecipitate of control tissues. Standard, ApoE (30 ng).

protein (APP; top band, calculated molecular weight 87.1 kDa), dimer, trimer, and multimeric  $A\beta$ , were identified in all AD samples (anti- $A\beta$ , lanes 2–5). In samples from the control subject (anti- $A\beta$ , lanes 6–7), the APP band was detected in both hippocampus and cortex (anti- $A\beta$ , lane 6 and 7), while dimer and trimer of  $A\beta$  were just identified in the hippocampus (anti- $A\beta$ , lane 6). Immunodetection with rabbit anti-human Hpt antibody demonstrated the presence of Hpt chains in all brain tissues (Figure 4, panel A, anti-Hpt).

To verify whether Hpt binds  $A\beta$  in human brain, hippocampus and cortex of the two AD patients or of the control subject were pooled and Hpt was immunoprecipitated. After 4–20% PAGE-D and Western blotting, we found that  $A\beta$  dimer, trimer, and multimers (Figure 4, panel B, anti- $A\beta$ ) as well as ApoE (Figure 4, panel B, anti-ApoE) were coimmunoprecipitated with Hpt. The amount of the  $A\beta$ -containing epitopes immunoprecipitated with Hpt was, as

expected, higher in the pool of brain tissues from AD patients than in the pool from the healthy subject (Figure 4).

The hypothesis that Hpt simultaneously interacts with  $A\beta$  and ApoE was also explored by immunoprecipitating Hpt in CSF from AD patients and healthy subjects. In particular, as we found a wide range of Hpt concentration in CSF from AD patients (0.56–4.57  $\mu\text{g}/\text{mL}$ ), we analyzed two AD pools with different Hpt titer, but similar ApoE concentration (pool 1,  $N = 6$ ; ApoE concentration  $2.688 \pm 0.373 \mu\text{g}/\text{mL}$ , Hpt concentration  $0.645 \pm 0.076 \mu\text{g}/\text{mL}$ ; pool 2,  $N = 8$ ; ApoE concentration  $2.106 \pm 0.326 \mu\text{g}/\text{mL}$ , Hpt concentration  $2.264 \pm 0.344 \mu\text{g}/\text{mL}$ ), and one pool from healthy subjects ( $N = 5$ ; ApoE concentration  $1.192 \pm 0.028 \mu\text{g}/\text{mL}$ , Hpt concentration  $0.518 \pm 0.058 \mu\text{g}/\text{mL}$ ). Since endogenous  $A\beta$  was not detectable in CSF by Western blotting, each pool was supplemented with  $A\beta_{1-42}$  (0.5  $\mu\text{M}$  final concentration) and Hpt was immunoprecipitated by mouse anti-Hpt IgG. As shown in Figure 5,  $A\beta$  (panel A), ApoE (panel B), and the

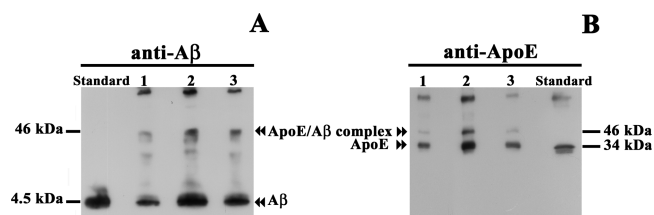


**Figure 5.** Immunoprecipitation of Hpt in CSF. Aliquots (100  $\mu\text{L}$ ) of two CSF pools from AD patients, with different endogenous Hpt concentration, and an aliquot of a CSF pool from healthy subjects were supplemented with 0.5  $\mu\text{M}$   $A\beta_{1-42}$ , and then immunoprecipitated by mouse anti-Hpt IgG. Samples were analyzed by 4–20% PAGE-D and Western blotting. Immunodetection was carried out with rabbit anti- $A\beta$  IgG, followed by GAR-HRP IgG (A) or with goat anti-ApoE IgG, followed by RAG-HRP IgG (B). Standard,  $A\beta_{1-42}$  (100 ng; panel A) or ApoE (100 ng; panel B). Lane 1, immunoprecipitate of AD-CSF with lower Hpt concentration. Lane 2, immunoprecipitate of AD-CSF with higher Hpt concentration. Lane 3, immunoprecipitate of healthy-CSF pool. In each panel, a single representative of at least three independent experiments is shown.

ApoE/ $A\beta$  complex (46 kDa band, panel A and B) coimmunoprecipitated with Hpt, thus supporting the hypothesis that Hpt,  $A\beta$ , and ApoE interact with each other in biological samples such as CSF. Lower amounts of  $A\beta$  and ApoE were detected in the immunoprecipitate from the pool of AD samples with lower Hpt concentration (lane 1) compared to the pool of AD samples with higher Hpt concentration (lane 2). Interestingly, a lower amount of the SDS-stable ApoE/ $A\beta$  complex was found in immunoprecipitate from AD with lower Hpt concentration than that from AD with higher Hpt concentration (lane 2). This led us to hypothesize that Hpt might promote the formation of the ApoE/ $A\beta$  complex.

**Hpt Effect on the Binding of ApoE to  $A\beta$ .** The influence of Hpt on ApoE binding to  $A\beta$  was explored by incubating  $A\beta$  with increasing amounts (0.001–0.1  $\mu\text{M}$ ) of LipoE2, LipoE3, or LipoE4 or with equimolar mixtures of each LipoE isoform and Hpt (0.001–0.1  $\mu\text{M}$ ). In all experimental conditions, the amount of ApoE bound to  $A\beta_{1-40}$  (Figure 6, panels A–C) or to  $A\beta_{1-42}$  (Figure 6, panels D–F) increased with the concentration of the apolipoprotein in the incubation medium. When Hpt was present in the incubation mixture with LipoE2 or LipoE3, the amount of LipoE bound to  $A\beta_{1-40}$  was found to be significantly higher ( $p < 0.01$ ; Figure 6, panels A and B,

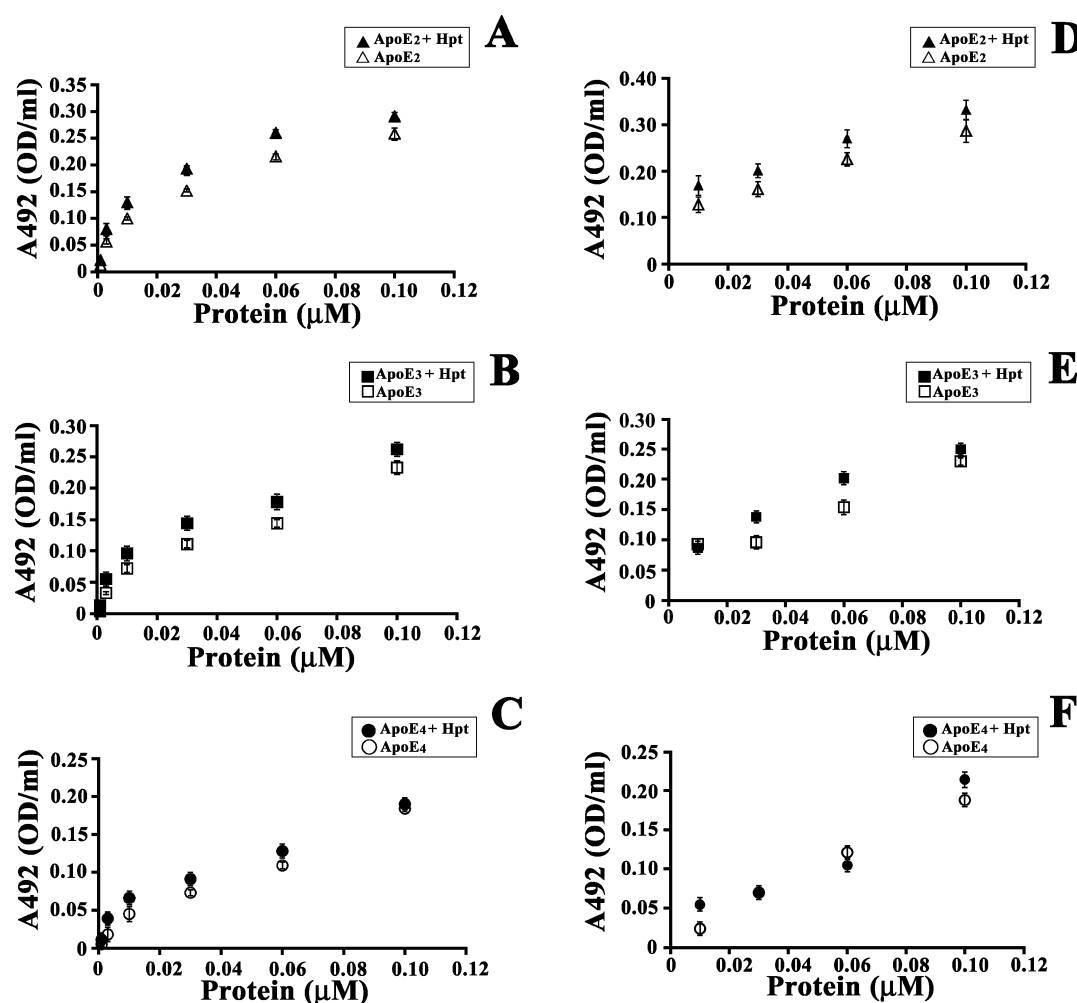


**Figure 6.** Effect of Hpt on ApoE binding to  $A\beta$ .  $A\beta_{1-40}$  or  $A\beta_{1-42}$  ( $0.22 \mu\text{M}$ )-coated wells were incubated with different amounts ( $0.001$ – $0.1 \mu\text{M}$ ) of liposome-embedded ApoE (LipoE2, LipoE3, or LipoE4; open symbols) or with equimolar mixtures of LipoE and Hpt 1-1 ( $0.001$ – $0.1 \mu\text{M}$ ; full symbols). ApoE bound to  $A\beta$  was detected by using goat anti-ApoE and RAG-HRP IgGs. Samples were analyzed in triplicate, and absorbance values (OD/mL) at 492 nm were expressed as mean  $\pm$  SEM. (A–C) Binding of LipoE2 (triangles), LipoE3 (squares), and LipoE4 (circles) to  $A\beta_{1-40}$ , respectively. (D–F) Binding of LipoE2, LipoE3, and LipoE4 to  $A\beta_{1-42}$ , respectively. In each panel, a single representative of at least three independent experiments is shown.

respectively), while no significant differences were found when Hpt was added in the incubation mixture with LipoE4 (Figure 6, panel C). A similar result was obtained with respect to  $A\beta_{1-42}$  (Figure 6, panels D–F). These data show that Hpt, at equimolar concentration with ApoE, improves the binding of E2 and E3 isoforms to  $A\beta$ .

The influence of Hpt on the formation of the complex between either LipoE isoform and  $A\beta_{1-42}$  or  $A\beta_{1-40}$  was further evaluated by Western blotting. In particular  $A\beta_{1-42}$  ( $10 \mu\text{M}$ ; Figure 7, panel A), or  $A\beta_{1-40}$  ( $10 \mu\text{M}$ ; Figure 7, panel B) was incubated with LipoE2 or LipoE3 or LipoE4 ( $0.5 \mu\text{M}$ ), and different amounts of Hpt ( $0.5$  or  $1.5 \mu\text{M}$ ). Samples were then analyzed by 4–20% PAGE-D, and Western blotting, and the ApoE/ $A\beta$  SDS-stable complex of 46 kDa was detected by incubation with mouse anti- $A\beta$  IgG 6E10. The densitometric analysis of the ApoE/ $A\beta$  complexes revealed that the amount of the ApoE/ $A\beta$  complex significantly increased ( $p < 0.01$ ) by increasing the Hpt/ApoE ratio in the mixture, thus suggesting that Hpt might promote the formation of the complex. In particular, the higher effect of Hpt was observed on the complex between  $A\beta$  and ApoE4, which is the isoform known to bind worse to the peptide. As a matter of fact, LipoE4/ $A\beta$

complex was not even ( $A\beta_{1-42}$ , Figure 7, panel A) or poorly detectable ( $A\beta_{1-40}$ , Figure 7, panel B), in the absence of Hpt, while its amount significantly increased in the presence of Hpt (11-fold and 59-fold for the LipoE4/ $A\beta_{1-42}$  complex in the presence of  $0.5$  and  $1.5 \mu\text{M}$  Hpt, respectively;  $p < 0.001$ ; 1.3-fold and 4-fold for the LipoE4/ $A\beta_{1-40}$  complex in the presence of  $0.5$  and  $1.5 \mu\text{M}$  Hpt, respectively;  $p < 0.001$ ). Altogether, our results suggest that Hpt, due to its ability to bind ApoE and  $A\beta$ , might facilitate the formation of the ApoE/ $A\beta$  complex.

**ApoE/ $A\beta$  Complex Formation in Conditioned Medium from 7PA2 Cell Line.** The effect of Hpt on the formation of the ApoE/ $A\beta$  complex was further investigated by using the 7PA2 cell line as source of endogenously produced, natural, and biologically relevant  $A\beta$  peptides. LipoE2, LipoE3, or LipoE4 ( $0.5 \mu\text{M}$ ) and different amounts of Hpt ( $0$ – $1.5 \mu\text{M}$ ) were added to the conditioned medium of 7PA2 cells (95% confluence; see Methods) and further incubated for 6 h. Medium from 7PA2 not exposed to Hpt was regarded as control. Media samples were then analyzed by 4–20% PAGE-D and Western blotting, and antigens containing  $A\beta$  epitopes were detected by incubation with mouse anti- $A\beta$  IgG 6E10.

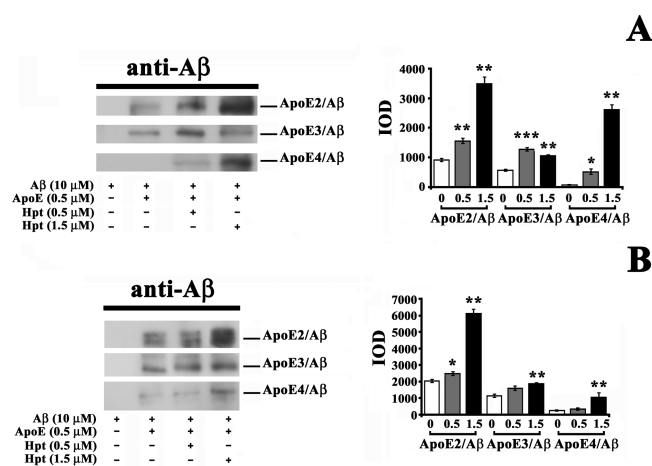


**Figure 7.** Influence of Hpt on the complex between synthetic  $A\beta$  and ApoE2, ApoE3, or ApoE4.  $A\beta_{1-42}$  (10  $\mu\text{M}$ ; panel A) or  $A\beta_{1-40}$  (10  $\mu\text{M}$ ; panel B) was incubated (20 h, 37  $^{\circ}\text{C}$ ) with LipoE2, LipoE3, or LipoE4 (0.5  $\mu\text{M}$ ), in the presence of different amounts of Hpt. Samples were analyzed by 4–20% PAGE-D and Western blotting. Immunocomplexes were detected by using mouse anti- $A\beta$  and GAM-HRP IgGs. Densitometric analysis of the complex detected by anti- $A\beta$  is shown. For densitometric measurements, samples were analyzed in triplicate, and data are expressed as mean  $\pm$  SEM. In each panel, a single representative of at least three independent experiments is shown. \* =  $p < 0.05$  versus control (incubation without Hpt); \*\* =  $p < 0.01$  versus control; \*\*\* =  $p < 0.001$  versus control.

As shown in Figure S3 (lane 2)  $A\beta$  monomers, dimers, and trimers, as well as soluble APP (sAPP) were detected, by anti- $A\beta$  immunostaining, in conditioned medium obtained in our experimental condition from 7PA2 cells. Further, the ApoE/ $A\beta$  complex was not even detectable in conditioned medium from 7PA2 cells, and poorly detectable when either ApoE isoform was added to the medium (Figure 8). The densitometric analysis of the ApoE/ $A\beta$  complexes demonstrated that Hpt addition to the medium significantly promoted the formation of the complex ( $p < 0.01$ ). In particular, accordingly with results obtained with synthetic  $A\beta$ , the higher effect of Hpt was observed in the presence of ApoE4. Indeed, the amount of LipoE4/ $A\beta$  complex significantly increased in the presence of Hpt (15-fold and 12-fold in the presence of 0.5 and 1.5  $\mu\text{M}$  Hpt respectively; Figure 8, panel C;  $p < 0.001$ ). The effect of 0.5  $\mu\text{M}$  Hpt (Hpt/ApoE ratio = 1) on the formation of the complex did not differ between ApoE2 and ApoE3 (3-fold increase;  $p < 0.01$ ), while the effect of 1.5  $\mu\text{M}$  Hpt (Hpt/ApoE ratio = 3) was higher on ApoE3 (11-fold increase;  $p < 0.001$ ) than on ApoE2 (4-fold increase;  $p < 0.001$ ). These results confirm that Hpt positively influences the interaction of ApoE with  $A\beta$ , also when the peptide is endogenously produced by a cellular model of AD, and strongly support the hypothesis that Hpt might mediate intermolecular interactions between ApoE and  $A\beta$  or contribute to the acquisition of a specific conformation of ApoE or  $A\beta$ , thus promoting the formation of the complex.

## DISCUSSION

AD and other neurodegenerative diseases may be enabled by specific aging- or inflammation-related factors, such as gradual failure of neuroprotective mechanisms or protein clearance.<sup>33,34</sup> We previously demonstrated that Hpt binds ApoE and impairs both the stimulation of this apolipoprotein on the activity of lecithin/cholesterol acyl transferase enzyme and the delivery of

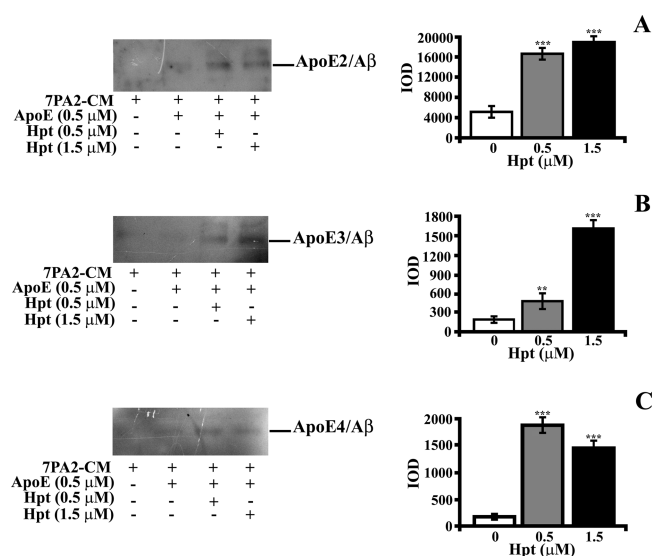


**Figure 8.** Influence of Hpt on the complex between naturally occurring  $A\beta$  and ApoE2, ApoE3, or ApoE4. The 7PA2 cell line was used as the source of endogenously produced  $A\beta$  peptides. 7PA2 cells were seeded into 6-well plates (350 000 cells/well) in complete medium and grown to about 95% confluence (48 h). After medium removal, cells were washed and then incubated in serum-free DMEM for 16 h. LipoE2, LipoE3, or LipoE4 (0.5  $\mu\text{M}$ ) was then added to the wells, in the presence of different amounts of Hpt 1–1 (0, 0.5, or 1.5  $\mu\text{M}$ ), and further incubated for 6 h. Media samples were then analyzed by 4–20% PAGE-D and Western blotting. Immunocomplexes were detected by using mouse anti- $A\beta$  and GAM-HRP IgGs. Densitometric analysis of the complex detected by anti- $A\beta$  is shown. For densitometric measurements, samples were analyzed in triplicate, and data are expressed as mean  $\pm$  SEM. In each panel, a single representative of at least three independent experiments is shown. \*\* =  $p < 0.01$  versus control (incubation without Hpt); \*\*\* =  $p < 0.001$  versus control.

lipoproteins to hepatocytes.<sup>9</sup> Hpt is a pleiotropic protein,<sup>11</sup> but limited studies are available on its role in brain in physiological or pathological conditions. As a different prevalence of Hpt phenotypes in several diseases, including AD, was shown,<sup>28,35</sup> we first analyzed the ability of each Hpt phenotype to bind both  $A\beta_{1-40}$  and  $A\beta_{1-42}$ . Our results demonstrate that the three Hpt phenotypes bind  $A\beta$  peptides with similar efficiency, thus suggesting that this interaction might mainly depends on Hpt  $\beta$  chain, which is also involved in the binding to Hb.<sup>12</sup> This hypothesis was supported by the finding that  $A\beta$  competes with Hb for the binding to Hpt. After trauma and cerebrovascular injuries, increased levels of free Hb mediate deleterious effects to the central nervous system.<sup>16</sup> Indeed, pathological and epidemiological evidence supports the association between capillary hemorrhage, amyloid deposition, and plaque formation.<sup>36,37</sup>  $A\beta$ , when present in a molar excess over Hb, might impair the antioxidant function of Hpt, which captures and neutralizes free Hb.

Further, we report here that Hpt forms an SDS-stable complex with  $A\beta$ . The ability of Hpt to bind ApoE and  $A\beta$  in vivo was demonstrated by coimmunoprecipitation of these proteins with Hpt in brain tissues from AD patients. The interaction of Hpt with  $A\beta$  might be critical not only for impairing peptide fibrillation<sup>22</sup> and accumulation, but also for participating to  $A\beta$  homeostasis by promoting peptide uptake in astrocytes or microglia, or its elimination through the blood-brain barrier.

We previously published that Hpt binds an ApoE domain localized in helix 4 of the N-terminal region,<sup>38</sup> whereas the ApoE binding site for A $\beta$  is in the C-terminal domain.<sup>39,40</sup> Hence, it cannot be excluded that ApoE binds both Hpt and A $\beta$ . Interestingly, we found that the interaction of Hpt with ApoE does not impair the binding of the apolipoprotein to A $\beta$ . Indeed, Hpt does not compete with A $\beta$  for the binding to ApoE, also when present in a 10-fold molar excess over the apolipoprotein. Moreover, our experiments carried out with CSF from AD patients and healthy subjects, showed that ApoE, A $\beta$ , and the ApoE/A $\beta$  complex coimmunoprecipitate with Hpt. Although CSF supplementation with exogenous A $\beta$  does not perfectly mimic a physiological condition, the results demonstrate that Hpt interacts with A $\beta$  and ApoE not only in experimental conditions based on the use of ApoE-liposome, but also in biological samples containing endogenous Hpt and ApoE. The mutual interaction between the three ligands was further confirmed by the finding of higher amounts of ApoE, A $\beta$ , and ApoE/A $\beta$  complex in the immunoprecipitate from AD CSF with higher Hpt concentration.

Intriguingly, ELISA experiments demonstrated that Hpt, in equimolar concentration with ApoE, significantly improves the binding of the apolipoprotein to A $\beta$  peptide. This was further supported by Western blotting showing that Hpt enhances the formation of the ApoE/A $\beta$  complex, when commercial synthetic peptide or A $\beta$  endogenously produced by the AD cell model 7PA2 was used. The dose-dependent influence of Hpt on the formation of ApoE/A $\beta$  complex suggests that a cooperative effect might exist. It is worth mentioning that the ApoE/A $\beta$  complex was shown to be crucial for preventing or limiting A $\beta$  neurotoxicity<sup>41</sup> and for promoting A $\beta$  clearance via ApoE receptors.<sup>41–43</sup> Interestingly, our results, from cell biology and biochemical experiments, showed that the effect of Hpt was more pronounced just in the presence of ApoE4 isoform. As ApoE4 causally contributes to AD pathogenesis,<sup>2</sup> Hpt increase in brain might overcome the inherent lower activity of ApoE4, by promoting its binding to A $\beta$ . To our knowledge, Hpt is the first identified molecule able to improve the binding between ApoE and A $\beta$ . We postulate that Hpt might work as a bridge between the two proteins, bringing them closer to each other (Figure S4). Alternatively, Hpt, as binding both ApoE and A $\beta$ , might influence molecular conformation of these two ligands in such a way that increases the chance for ApoE and A $\beta$  to interact with each other.

In conclusion, we suggest that Hpt might represent a new player in the crosstalk between ApoE and A $\beta$ . Although several questions remain to be answered, concerning the structural requirement for the assembly of Hpt, ApoE, and A $\beta$ , and the physiological effect on target mechanisms, this work provides a framework for future mechanistic studies on the functioning of this chaperoning pathway. The risk of developing AD might not only be linked to the presence of different ApoE isoforms or limited to specific ApoE effects on lipid or A $\beta$  metabolism, but also rely on the level of critical ligands, such as Hpt, able to influence ApoE/A $\beta$  interaction and/or ApoE functions.

## METHODS

**Materials.** Bovine serum albumin fraction V (BSA), gelatin, lecithin, Hb, Tissue Protease Inhibitor Cocktail, rabbit anti-human Hpt IgG, goat anti-rabbit horseradish peroxidase-conjugated IgG (GAR-HRP), and goat anti-mouse horseradish peroxidase-conjugated IgG (GAM-HRP) were purchased from Sigma-Aldrich (St. Louis, MO). Recombinant human ApoE2, ApoE3, and ApoE4 were from

PeptoTech (London, U.K.). Goat anti-human ApoE IgG, rabbit anti-goat horseradish peroxidase-conjugated IgG (RAG-HRP), protein G Plus/protein A agarose suspension, and centrifugal filter device Amicon Ultra (3 kDa cutoff) were from Merk Millipore (Merk Chemicals Limited, Nottingham, U.K.). Mouse anti-human ApoE IgG was from Santa Cruz Biotechnology (Santa Cruz, CA). A $\beta$  peptides were from INBIOS s.r.l. (Naples, Italy). Mouse antibody 6E10 (against A $\beta$  residues 1–16) was from Covance (Princeton, NJ). The dye reagent for protein titration, enhanced chemiluminescence (ECL) reagents, and the polyvinylidene difluoride (PVDF) membrane were from Bio-Rad (Bio-Rad, Hercules, CA). Polystyrene 96-well ELISA MaxiSorp plates, with high affinity to proteins with mixed hydrophilic/hydrophobic domains, were purchased from Nunc (Roskilde, Denmark). Kodak Biomax light film and Sephacryl S-200, CNBr-activated Sepharose 4 Fast Flow, and Blue Sepharose 6 Fast Flow resins were from GE-Healthcare Life Sciences (Milano, Italy).

Dulbecco's modified Eagle's medium (DMEM) and fetal bovine serum (FBS) were from BioWhittaker (Verseviere, Belgium). L-Glutamine, penicillin, and streptomycin were from Gibco (Life Technologies Italy, Monza, Italy). Antibiotic G-418 sulfate solution was from Promega Italia (Milan, Italy). Cell culture flasks (75 cm<sup>2</sup>), 6-well cell culture plates, and sterile pipets from Beckton-Dickinson (Milan, Italy) were used.

**Cell Culture.** The 7PA2 cell line was kindly provided by Dr. Denis Selkoe (Harvard Medical School, Boston, MA). 7PA2 cells are CHO stably transfected with the human APP751 cDNA bearing the V717F fAD mutation,<sup>27</sup> and represent the best characterized model of naturally occurring A $\beta$  peptides.<sup>25,26,44,45</sup> Cells ( $1.5 \times 10^6$ ) were seeded in T-75 tissue culture flasks (75 cm<sup>2</sup> surface) and grown in DMEM with 10% FBS, 2 mM L-glutamine, 100 U/mL penicillin, 100  $\mu$ g/mL streptomycin, and 300  $\mu$ g/mL antibiotic selection G418 (complete medium) at 37 °C and under humidified atmosphere of 5% CO<sub>2</sub> in air, as previously described.<sup>45</sup> The medium was changed three times a week, and cells were subcultivated when confluent.

To obtain conditioned medium (CM), 7PA2 cells were seeded into 6-well plates (at 350 000 cells/well density) in complete medium and grown (37 °C, 5% CO<sub>2</sub>) to about 95% confluence (48 h). Cells were then washed (twice) with DMEM and then incubated for 16 h in 1100  $\mu$ L of DMEM containing 2 mM L-glutamine, 100 U/mL penicillin, and 100  $\mu$ g/mL streptomycin. Anti-A $\beta$  immunostaining of conditioned medium is shown in Figure S3.

**CSF and Brain Tissues.** CSF from healthy subjects ( $N = 5$ ), matched for age (range: 40–50 years), were provided by P. Bongioanni (Pisa, Italy). CSF from AD patients ( $N = 14$ ), matched for age (range: 60–70 years), were provided by the Department of Experimental Biomedicine and Clinical Neurosciences (University of Palermo, Italy). Human brain tissues from two patients with post-mortem confirmed AD and from a healthy age-matched control subject were provided by Centro Regionale di Neurogenetica (Lamezia, CT, Italy). The healthy subject died from accidental intracerebral bleeding in the left brain hemisphere, and the sample was taken from the contralateral brain hemisphere. All brain donors or their legal tutors gave written informed consent during their lifetimes and the protocol was approved by the local Ethics Committee. The study conforms to The Code of Ethics of the World Medical Association (Declaration of Helsinki), printed in the British Medical Journal (18 July 1964), and it was approved by the Ethics Committee of the University of Naples Federico II.

**ELISA.** ApoE and Hpt concentration in individual CSF samples and in pooled samples from AD or healthy controls was measured by ELISA. Samples were diluted (1:100–1:800) with coating buffer (7 mM Na<sub>2</sub>CO<sub>3</sub>, 17 mM NaHCO<sub>3</sub>, 1.5 mM NaN<sub>3</sub>, pH 9.6) and incubated in the wells of a microtiter plate (Immuno MaxiSorp; overnight, 4 °C). After four washes with TBS (130 mM NaCl, 20 mM Tris-HCl, pH 7.4) containing 0.05% (v/v) Tween 20 (T-TBS) and four washes with high salt TBS (500 mM NaCl in 20 mM Tris-HCl at pH 7.4), the wells were blocked with TBS containing 0.5% BSA (1 h/37 °C). After washing, the wells were incubated (1 h, 37 °C) with 60  $\mu$ L of goat anti-ApoE IgG (1:3000 dilution in T-TBS containing 0.25% BSA), followed by 60  $\mu$ L of RAG-HRP IgG (1:14 000 dilution) for

immunodetection of ApoE, or with 60  $\mu$ L of rabbit anti-Hpt IgG (1:1500 dilution), followed by GAR-HRP IgG (1:8000 dilution) for Hpt detection. Peroxidase-catalyzed color development from *o*-phenylenediamine was measured at 492 nm.<sup>9</sup>

**Purification of Hpt.** Hpt was isolated from plasma of healthy subjects (phenotype 2-1, 2-2, or 1-1) by a multistep purification procedure, based on a gel filtration with a column of Sephacryl S-200, followed by an affinity chromatography with a column of Blue Sepharose 6 Fast Flow, and finally by a further purification by affinity chromatography using a Sepharose resin coupled to anti-Hpt IgG.<sup>9</sup> Hpt was over 98% pure, as assessed by SDS-PAGE and densitometric analysis of Coomassie-stained bands. The molarity of each Hpt phenotype was determined by measuring the protein concentration<sup>46</sup> and calculating the molecular weight of the monomer  $\alpha\beta$  as previously described.<sup>47</sup>

**A $\beta$  Preparation.** Human A $\beta_{1-40}$  and A $\beta_{1-42}$  (purity > 95% as assessed by HPLC) were produced by chemical synthesis. To obtain a solution free of aggregates and fibrils, the lyophilized peptide was treated with 1,1,1,3,3,3-hexafluoro-2-propanol (HFIP).<sup>48</sup> After HFIP evaporation under nitrogen stream, A $\beta$  was stored desiccated at -20 °C. The peptide was resuspended in anhydrous dimethyl sulfoxide prior to use and sonicated for 20 min (bath sonicator model 3200MH; Soltec), and its concentration was verified by a colorimetric assay<sup>46</sup> using insulin as standard for calibration.

**Binding of Hpt to A $\beta$ .** The wells of a microtiter plate were coated with 50  $\mu$ L of A $\beta_{1-40}$  or A $\beta_{1-42}$  (0.002 mg/mL in coating buffer; 0.45  $\mu$ M) and incubated overnight at 4 °C. Under these conditions, 22 ng/well of A $\beta$  bound to the wells (corresponding to 22% of the amount of the coated peptide). After four washes with T-TBS and four washes with high salt TBS for removing the excess of A $\beta$ , the wells were blocked with TBS containing 0.5% BSA (1 h, 37 °C). The wells were extensively washed, and then incubated (2 h, 37 °C) with different amounts (0.05, 0.15, 0.3, 0.5, 0.7, or 1  $\mu$ M in TBS) of each Hpt phenotype (2-1, 2-2, or 1-1). The amount of Hpt bound to A $\beta$  was measured by incubating the wells with 60  $\mu$ L of rabbit anti-Hpt IgG (1:2500 dilution in T-TBS containing 0.25% BSA; 1 h, 37 °C), followed by 60  $\mu$ L of GAR-HRP IgG (1:6000 dilution; 1 h, 37 °C). Color development was measured at 492 nm. Absorbance values were converted to the percentage of the value obtained with 1  $\mu$ M Hpt (assumed as 100% of Hpt binding to A $\beta$ ). Background values (nonspecific binding of Hpt to the wells or to BSA in the blocking solution) were measured in wells processed without A $\beta$  coating. Data were analyzed by using a nonlinear regression fit algorithm in GraphPad Prism v 5.01, to obtain the dissociation constant ( $K_d$ ) of each Hpt phenotype for A $\beta_{1-40}$  and A $\beta_{1-42}$ .

**Competition between A $\beta$  and Hb for Binding Hpt.** The wells of a microtiter plate were coated with 50  $\mu$ L of Hb (0.008 mg/mL in coating buffer; 0.125  $\mu$ M) and incubated overnight at 4 °C. Hb excess was removed by washing with T-TBS and with high salt TBS, and the remaining sites on the plate were blocked with TBS containing 0.5% BSA (1 h, 37 °C). After extensive washing, aliquots (50  $\mu$ L) from mixtures containing 0.3  $\mu$ M Hpt 2-1, Hpt 2-2, or Hpt 1-1 and different concentrations of A $\beta_{1-40}$  or A $\beta_{1-42}$  (0, 1, 3, 6, 8, or 10  $\mu$ M in TBS) were incubated (2 h, 37 °C) into Hb-coated wells. Hpt bound to Hb was detected by treatment with anti-Hpt IgG (1:2000 dilution; 1 h, 37 °C), followed by GAR-HRP IgG (1:6000 dilution; 1 h, 37 °C). Absorbance values were converted to the percentage of the value obtained in the absence of A $\beta$  (assumed as 100% of Hpt binding to Hb).

**Competition of Hpt with A $\beta$  for Binding to ApoE.** Liposomes containing ApoE2, ApoE3, or ApoE4 (ApoE/lecithin = 1:133 molar contribution; namely, LipoE2, LipoE3, or LipoE4) were prepared by the cholate dialysis method.<sup>38,49</sup> The wells were coated with 50  $\mu$ L of 0.001 mg/mL A $\beta_{1-40}$  or A $\beta_{1-42}$  (0.23  $\mu$ M) and incubated overnight at 4 °C. Under these conditions, 9 ng/well of peptide bound to the wells (18% of the peptide offered). A $\beta$  excess was removed by washing with T-TBS and with high salt TBS, and the wells were blocked with PBS containing 1% BSA and 1% gelatin (2 h, 37 °C). The wells were then incubated (2 h, 37 °C) with aliquots (55  $\mu$ L) from mixtures containing 0.010  $\mu$ M LipoE2, LipoE3, or LipoE4 and different concentrations of

Hpt 1-1 (0, 0.005, 0.01, 0.03, 0.06, or 0.1  $\mu$ M). The amount of LipoE bound to A $\beta$  was measured by treatment with goat anti-ApoE IgG (1:2500 dilution in TBS; 1 h, 37 °C), followed by RAG-HRP IgG (1:7000 dilution in TBS; 1 h, 37 °C), and color development at 492 nm. Absorbance values were converted to the percent of the value obtained in the absence of Hpt (assumed as 100% of LipoE binding).

**Hpt/A $\beta$  Complex Formation.** Mixtures containing Hpt 1-1 (3  $\mu$ M), A $\beta_{1-40}$  (220  $\mu$ M), or Hpt 1-1 and A $\beta_{1-40}$  (3 and 220  $\mu$ M in PBS, respectively) were incubated 6 h at 37 °C. Experimental conditions (A $\beta$  concentration, time of incubation) were chosen according to those used for detecting ApoE/A $\beta$  complex.<sup>3,24</sup> Samples were treated with 3 $\times$  O'Farrell buffer, without  $\beta$ -mercaptoethanol,<sup>47</sup> boiled for 5 min, centrifuged for 5 min at 8000g, and then analyzed by 4–20% PAGE-D and Western blotting. In detail, proteins were transferred onto a PVDF membrane (1 h, under electric field), and the membrane was rinsed in T-TBS and then blocked with T-TBS containing 5% nonfat milk (overnight, 4 °C). The membrane was then incubated (1 h, 37 °C) with mouse anti-A $\beta$  IgG 6E10 (1:800 dilution in T-TBS containing 0.25% nonfat milk), followed by GAM-HRP IgG (1:2000 dilution; 1 h, 37 °C), for revealing antigens containing A $\beta$  epitopes, or with rabbit anti-Hpt IgG (1:2000 dilution; 1 h, 37 °C), followed by GAR-HRP IgG (1:4500 dilution; 1 h, 37 °C), for revealing antigens containing Hpt epitopes. The immunocomplexes were detected by using the ECL detection system, using luminol as substrate, according to the manufacturer's protocol.

The interaction between Hpt and A $\beta$  was further analyzed with lower concentrations of both proteins by incubating (20 h, 37 °C) mixtures containing A $\beta_{1-40}$  or A $\beta_{1-42}$  (10  $\mu$ M) and Hpt 1-1 (0.5 or 10  $\mu$ M). Samples were then analyzed by 4–20% PAGE-D and Western blotting. In particular, after blocking, the membrane was incubated with anti-A $\beta$  IgG 6E10 (1:500 dilution; overnight, 4 °C), followed by GAM-HRP IgG (1:1500 dilution; 1 h, 37 °C), or with rabbit anti-Hpt IgG (1:1000 dilution; overnight, 4 °C), followed by GAR-HRP IgG (1:4500 dilution, 1 h, 37 °C).

Samples of brain tissues homogenates (hippocampus and cortex) from two AD patients were pooled, and aliquots (50  $\mu$ g) of the pool were processed by 4–20% PAGE-D and Western blotting, as described above, for detecting antigens containing A $\beta$  and Hpt epitopes. Membrane probing was carried out with anti-A $\beta$  IgG 6E10 (1:500 dilution; overnight, 4 °C), followed by GAM-HRP IgG (1:15 000 dilution; 1 h, 37 °C), or with rabbit anti-Hpt IgG (1:500 dilution; overnight, 4 °C), followed by GAR-HRP IgG (1:15 000 dilution; 1 h, 37 °C).

The effect of time of incubation and Hpt concentration on the formation of Hpt/A $\beta$  complex was investigated by incubating (2 or 6 h, 37 °C) reaction mixtures containing A $\beta_{1-40}$  (220  $\mu$ M) and different amounts of Hpt 1-1 (3, 8, or 16  $\mu$ M). Samples were boiled for 5 min and processed for 4–20% PAGE-D and Western blotting. The immunodetection was performed with mouse anti-A $\beta$  IgG 6E10 (1:800 dilution; 1 h, 37 °C), followed by GAM-HRP IgG (1:2000 dilution; 1 h, 37 °C), for detecting antigens containing A $\beta$  epitopes, or with rabbit anti-Hpt IgG (1:2000 dilution; 1 h, 37 °C), followed by GAR-HRP IgG (1:4500 dilution; 1 h, 37 °C), for detecting antigens containing Hpt epitopes.

**Hpt Influence on the Ability of ApoE to Bind A $\beta$ .** The wells of a microtiter plate were coated with 50  $\mu$ L of 0.001 mg/mL A $\beta_{1-40}$  or A $\beta_{1-42}$  (overnight, 4 °C). A $\beta$  excess was removed by washing with T-TBS and with high salt TBS, and the remaining sites were blocked with PBS containing 1% BSA and 1% gelatin (2 h, 37 °C). After washing, the wells were incubated (2 h, 37 °C) with different amounts (0.001, 0.003, 0.01, 0.03, 0.06, or 0.1  $\mu$ M in TBS) of LipoE2, LipoE3, or LipoE4, or with equimolar mixtures of LipoE and Hpt (0.001, 0.003, 0.01, 0.03, 0.06, or 0.1  $\mu$ M in TBS). ApoE bound to A $\beta$  was detected by incubation with goat anti-ApoE IgG (1:6000 dilution in TBS; 1 h, 37 °C), followed by RAG-HRP IgG (1:50 000; 1 h, 37 °C), and color development at 492 nm.

**Analysis of Human Brain Homogenates.** Post-mortem brain tissues (hippocampus and prefrontal cortex) from two AD subjects and one control subject were homogenized in three volumes (w/v) of cold RIPA buffer (150 mM NaCl, 50 mM Tris-HCl, 1% Nonidet P-40,



0.5% sodium deoxycholate, pH 8) containing Tissue Protease Inhibitor Cocktail (1:200, v/v). Homogenates were centrifuged (140 00g, 45 min, 4 °C), and protein concentration of supernatants was measured.<sup>46</sup> Aliquots (50 µg) of hippocampus and cortex from each sample were processed by 4–20% PAGE-D and Western blotting for verifying the presence of Aβ epitopes. In particular, after blocking with T-TBS containing 5% nonfat milk (1 h, 37 °C), the membrane was incubated with mouse anti-Aβ IgG 6E10 (1:500 dilution in T-TBS containing 0.25% nonfat milk; overnight, 4 °C), followed by GAM-HRP IgG (1:5000 dilution; 1 h, 37 °C). The immunocomplexes were detected by using the ECL detection system.

Samples of brain tissues (hippocampus and cortex) from each subject were pooled and aliquots (50 µg) were analyzed by 15% SDS PAGE, under reducing conditions, and Western blotting, for revealing Hpt epitopes. After blocking (1 h, 37 °C), the membrane was incubated with rabbit anti-Hpt IgG (1:500 dilution; overnight, 4 °C), followed by GAR-HRP IgG (1:10 000 dilution; 1 h, 37 °C).

**Immunoprecipitation of Hpt in Human Brain.** The analysis of interaction between Hpt and Aβ or ApoE was performed on pools of hippocampus and cortex, from AD patients or control subject, by immunoprecipitating Hpt. In detail, each pool (160 µg of total protein) was incubated (overnight, 4 °C) with rabbit anti-Hpt IgG and then with 60 µL of protein G Plus/protein A agarose suspension (2 h, 4 °C). Immunoprecipitates were collected by centrifugation (10 min, 300g), washed with TBS containing 0.05% SDS, fractionated by 4–20% PAGE-D, and finally blotted onto a PVDF membrane. The membrane was blocked as described above and then incubated with mouse anti-Aβ IgG 6E10 (1:500 dilution; overnight, 4 °C), followed by GAM HRP IgG (1:5000 dilution; 1 h, 37 °C), for detection of Aβ-containing antigens, or with goat anti-ApoE IgG (1:500 dilution; 1 h, 37 °C), followed by RAG HRP IgG (1:12 000 dilution; 1 h, 37 °C), for detection of ApoE-containing epitopes.

**Immunoprecipitation of Hpt in CSF.** Immunoprecipitation of Hpt was also carried out in pooled CSF (each sample contributing with equal volume) of patients with AD or healthy subjects. In detail, aliquots (100 µL) of two AD CSF pools, with different Hpt concentration, but similar ApoE concentration (pool 1,  $N = 6$ ; ApoE concentration  $2.688 \pm 0.373$  µg/mL, Hpt concentration  $0.645 \pm 0.076$  µg/mL; pool 2,  $N = 8$ ; ApoE concentration  $2.106 \pm 0.326$  µg/mL, Hpt concentration  $2.264 \pm 0.344$  µg/mL), and an aliquot of a CSF pool from controls (pool 3,  $N = 5$ ; ApoE concentration  $1.192 \pm 0.028$  µg/mL, Hpt concentration  $0.518 \pm 0.058$  µg/mL) were supplemented with Aβ<sub>1–42</sub> (final concentration 0.5 µM) and then incubated for 5 h at 37 °C. Each sample was immunoprecipitated by incubation (overnight, 4 °C) with mouse anti-Hpt IgG, followed by addition of 20 µL of protein G Plus/protein A agarose suspension and further incubation (2 h, 4 °C). Immunoprecipitates were fractionated by 4–20% PAGE-D, and finally blotted onto PVDF membrane. The membrane was blocked as described above and then incubated with rabbit anti-Aβ IgG (1:650 dilution; 1 h, 37 °C), followed by GAR HRP IgG (1:7000 dilution; 1 h, 37 °C), for detection of Aβ-containing antigens, or with goat anti-ApoE IgG (1:750 dilution; 1 h, 37 °C), followed by RAG HRP IgG (1:12 000 dilution; 1 h, 37 °C), for detection of ApoE-containing epitopes. Immunodetection was carried out with Clarity Western ECL substrate.

**ApoE/Aβ Complex Formation in the Presence of Hpt.** Aβ<sub>1–40</sub> or Aβ<sub>1–42</sub> (10 µM) was incubated (20 h, 37 °C) with LipoE2, LipoE3, or LipoE4 (0.5 µM), in the presence of different amounts of Hpt 1-1 (0, 0.5, or 1.5 µM). Samples were analyzed by 4–20% PAGE-D and Western blotting as described above. After blocking, the membrane was incubated (1 h, 37 °C) with mouse anti-Aβ IgG 6E10 (1:2000 dilution), followed by GAM-HRP IgG (1:4000 dilution; 1 h, 37 °C), and ECL staining for revealing antigens containing Aβ epitopes. Quantitative densitometry of the ApoE/Aβ immunocomplexes was then carried out by analyzing the digital images of membranes by the Gel-Pro Analyzer software (Media Cybernetics, Silver Spring, MA). Band intensities are expressed as integrated optical density (IOD).

**ApoE/Aβ Complex Formation in Conditioned Medium from 7PA2 Cell Line.** 7PA2 cells were seeded into 6-well plates (at 350 000 cells/well density) in complete medium and grown to about 95%

confluence (48 h). Cells were washed (twice) with DMEM and then incubated for 16 h in DMEM containing 2 mM L-glutamine, 100 U/mL penicillin, and 100 µg/mL streptomycin. LipoE2, LipoE3, or LipoE4 (0.5 µM) was then added to the wells, in the presence of different amounts of Hpt 1-1 (0, 0.5, or 1.5 µM). After 6 h of incubation (37 °C, 5% CO<sub>2</sub>), cell culture supernatants were collected, treated with Tissue Protease Inhibitor Cocktail (Sigma-Aldrich, 1:200, v/v), and finally centrifuged at 400g for 5 min to remove any cellular debris. Supernatants from cells not exposed to Hpt were used as control. Media samples were then concentrated (three times) by centrifugation steps in centrifugal filter device Amicon Ultra (3 kDa cutoff, Merk Millipore). Aliquots (40 µL) of each sample were analyzed by 4–20% PAGE-D and Western blotting essentially as described above. In particular, protein transfer was performed (1 h, under electric field) onto nitrocellulose membrane filters (0.22 µm), and the membrane was boiled in PBS (3 min) after blotting, to increase the detection of low molecular weight bands.<sup>45</sup> After blocking, the membrane was incubated (overnight, 4 °C) with mouse anti-Aβ IgG 6E10 (1:500 dilution), followed by GAM-HRP IgG (1:1500 dilution; 1 h, 37 °C), and ECL staining. Quantitative densitometry of the ApoE/Aβ immunocomplexes was then carried out as described above.

**Statistical Analysis.** In all experiments, samples were processed in triplicate, and data were expressed as mean value ± SEM. The program “GraphPad Prism 5.01” (GraphPad Software, San Diego, CA) was used to perform regression analysis, Student’s *t* test, for comparing two groups of data, and one-way ANOVA, followed by Tukey’s test, for multiple group comparisons.  $P < 0.05$  was set as indicating significance.

## ■ ASSOCIATED CONTENT

### 📄 Supporting Information

Additional figures as described in the text. This material is available free of charge via the Internet at <http://pubs.acs.org>

## ■ AUTHOR INFORMATION

### Corresponding Author

\*Tel: +390812535244. Fax: +390812535090. E-mail: [luisa.cigliano@unina.it](mailto:luisa.cigliano@unina.it)

### Author Contributions

M.S.S. and L.C. conceived and designed the research, performed experiments, analyzed and interpreted all results, and wrote the manuscript. B.M., V.L.M., and A.C. performed experiments, analyzed data, and critically revised the manuscript. C.V. and P.A. contributed to the planning of experiments and critically revised the manuscript. C.C., T.P., R.G.M., and A.C.B. recruited AD patients and healthy subjects, collected CSF and brain tissues, and contributed to the execution of experiments.

### Funding

This research was supported by a grant from the Compagnia di San Paolo (Neuroscience Program; 3868 SD/SD–2008.2487).

### Notes

The authors declare no competing financial interest.

## ■ ACKNOWLEDGMENTS

The authors are grateful to Dr Fabrizio Dal Piaz for helpful discussion. The authors are thankful to Prof. Dennis Selkoe (Harvard Medical School, Boston) for providing 7PA2 cells. We wish to acknowledge Dr. Giovanni Meli (European Brain Research Institute, Roma, Italy) and Prof Antonino Cattaneo (Scuola Normale Superiore, Pisa, Italy) for their kind help.

## ■ ABBREVIATIONS

ApoE, apolipoprotein E; Hpt, haptoglobin; A $\beta$ , amyloid-beta; Hb, hemoglobin; CSF, cerebrospinal fluid; AD, Alzheimer's disease; LipoE, liposome-embedded ApoE; BSA, bovine serum albumin; GAM-HRP, goat anti-mouse horseradish peroxidase-conjugated IgG; GAR-HRP, goat anti-rabbit horseradish peroxidase-conjugated IgG; RAG-HRP, rabbit anti-goat horseradish peroxidase-conjugated IgG; HFIP, 1,1,1,3,3,3-hexafluoro-2-propanol; PVDF, polyvinylidene difluoride

## ■ REFERENCES

- (1) Hardy, J., and Selkoe, D. J. (2002) The amyloid hypothesis of Alzheimer's disease: progress and problems on the road to therapeutics. *Science* 297, 353–356.
- (2) Huang, Y., and Mucke, L. (2012) Alzheimer mechanisms and therapeutic strategies. *Cell* 148, 1204–1222.
- (3) Munson, G. W., Roher, A. E., Kuo, Y. M., Gilligan, S. M., Reardon, C. A., Getz, G. S., and LaDu, M. J. (2000) SDS-stable complex formation between native apolipoprotein E3 and beta-amyloid peptides. *Biochemistry* 39, 16119–16124.
- (4) Bentley, N. M., LaDu, M. J., Rajan, C., Getz, G. S., and Reardon, C. A. (2002) Apolipoprotein E structural requirements for the formation of SDS-stable complexes with beta-amyloid-(1–40): the role of salt bridges. *Biochem. J.* 366, 273–279.
- (5) Huang, Y. (2006) Molecular and cellular mechanisms of apolipoprotein E4 neurotoxicity and potential therapeutic strategies. *Curr. Opin. Drug Discovery Dev.* 9, 627–641.
- (6) Verghese, P. B., Castellano, J. M., and Holtzman, D. M. (2011) Apolipoprotein E in Alzheimer's disease and other neurological disorders. *Lancet Neurol.* 10, 241–252.
- (7) Mahley, R. W., and Rall, S. C., Jr. (2000) Apolipoprotein E: Far more than a lipid transport protein. *Annu. Rev. Genomics Hum. Genet.* 1, 507–537.
- (8) Rocchi, A., Pellegrini, S., Siciliano, G., and Murri, L. (2003) Causative and susceptibility genes for Alzheimer's disease: a review. *Brain Res. Bull.* 61, 1–24.
- (9) Cigliano, L., Pugliese, C. R., Spagnuolo, M. S., Palumbo, R., and Abrescia, P. (2009) Haptoglobin binds the antiatherogenic protein apolipoprotein E - Impairment of apolipoprotein E stimulation of both lecithin:cholesterol acyltransferase activity and cholesterol uptake by hepatocytes. *FEBS J.* 276, 6158–6171.
- (10) Yang, F., Haile, D. J., Berger, F. G., Herbert, D. C., Van Beveren, E., and Ghio, A. J. (2003) Haptoglobin reduces lung injury associated with exposure to blood. *Am. J. Physiol.: Lung Cell. Mol. Physiol.* 284, L402–409.
- (11) Quaye, I. K. (2008) Haptoglobin, inflammation and disease. *Trans. R. Soc. Trop. Med. Hyg.* 102, 735–742.
- (12) Langlois, M. R., and Delanghe, J. R. (1996) Biological and clinical significance of haptoglobin polymorphism in humans. *Clin. Chem.* 42, 1589–1600.
- (13) Chamoun, V., Zeman, A., Blennow, K., Fredman, P., Wallin, A., Keir, G., Giovannoni, G., and Thompson, E. J. (2001) Haptoglobin as markers of blood-CSF barrier dysfunction: the findings in normal CSF. *J. Neurol. Sci.* 182, 117–121.
- (14) Lee, M. Y., Kim, S. Y., Choi, J. S., Lee, I. H., Choi, Y. S., Jin, J. Y., Park, S. J., Sung, K. W., Chun, M. H., and Kim, I. S. (2002) Upregulation of haptoglobin in reactive astrocytes after transient forebrain ischemia in rats. *J. Cereb. Blood Flow Metab.* 22, 1176–1180.
- (15) Borsody, M., Burke, A., Coplin, W., Miller-Lotan, R., and Levy, A. (2006) Haptoglobin and the development of cerebral artery vasospasm after subarachnoid hemorrhage. *Neurology* 66, 634–640.
- (16) Zhao, X., Song, S., Sun, G., Strong, R., Zhang, J., Grotta, J. C., and Aronowski, J. (2009) Neuroprotective role of haptoglobin after intracerebral hemorrhage. *J. Neurosci.* 29, 15819–15827.
- (17) Johnson, G., Brane, D., Block, W., van Kammen, D. P., Gurklis, J., Peters, J. L., Wyatt, R. J., Kirch, D. G., Ghanbari, H. A., and Merrill, C. R. (1992) Cerebrospinal fluid protein variations in common to Alzheimer's disease and schizophrenia. *Appl. Theor. Electrophor.* 3, 47–53.
- (18) Argüelles, S., Venero, J. L., García-Rodríguez, S., Tomas-Camardiel, M., Ayala, A., Cano, J., and Machado, A. (2010) Use of haptoglobin and transthyretin as potential biomarkers for the preclinical diagnosis of Parkinson's disease. *Neurochem. Int.* 57, 227–234.
- (19) Huang, Y. C., Wu, Y. R., Tseng, M. Y., Chen, Y. C., Hsieh, S. Y., and Chen, C. M. (2011) Increased prothrombin, apolipoprotein A-IV, and haptoglobin in the cerebrospinal fluid of patients with Huntington's disease. *PLoS One* 6, e15809.
- (20) Powers, J. M., Schlaepfer, W. W., Willingham, M. C., and Hall, B. J. (1981) An immunoperoxidase study of senile cerebral amyloidosis with pathogenetic considerations. *J. Neuropathol. Exp. Neurol.* 40, 592–612.
- (21) Yerbury, J. J., Poon, S., Meehan, S., Thompson, B., Kumita, J. R., Dobson, C. M., and Wilson, M. R. (2007) The extracellular chaperone clusterin influences amyloid formation and toxicity by interacting with prefibrillar structures. *FASEB J.* 21, 2312–2322.
- (22) Yerbury, J. J., Kumita, J. R., Meehan, S., Dobson, C. M., and Wilson, M. R. (2009)  $\alpha$ 2-Macroglobulin and Haptoglobin Suppress Amyloid Formation by Interacting with Prefibrillar Protein Species. *J. Biol. Chem.* 284, 4246–4254.
- (23) Cocciolo, A., Di Domenico, F., Coccia, R., Fiorini, A., Cai, J., Pierce, W. M., Mecocci, P., Butterfield, D. A., and Perluigi, M. (2012) Decreased expression and increased oxidation of plasma haptoglobin in Alzheimer disease: Insights from redox proteomics. *Free Radical Biol. Med.* 53, 1868–1876.
- (24) LaDu, M. J., Falduto, M. T., Manelli, A. M., Reardon, C. A., Getz, G. S., and Frail, D. E. (1994) Isoform-specific binding of apolipoprotein E to beta-amyloid. *J. Biol. Chem.* 269, 23403–23406.
- (25) Portelius, E., Olsson, M., Brinkmalm, G., Ruetschi, U., Mattsson, N., Andreasson, U., Gobom, J., Brinkmalm, A., Holtta, M., Blennow, K., and Zetterberg, H. (2012) Mass spectrometric characterization of amyloid-beta species in the 7PA2 cell model of Alzheimer's disease. *J. Alzheimer's Dis.* 33, 85–93.
- (26) Walsh, D. M., Klyubin, I., Fadeeva, J. V., Cullen, W. K., Anwyl, R., Wolfe, M. S., Rowan, M. J., and Selkoe, D. J. (2002) Naturally secreted oligomers of amyloid beta protein potently inhibit hippocampal long-term potentiation in vivo. *Nature* 416, 535–539.
- (27) Podlisny, M. B., Ostaszewski, B. L., Squazzo, S. L., Koo, E. H., Rydell, R. E., Teplow, D. B., and Selkoe, D. J. (1995) Aggregation of secreted amyloid beta-protein into sodium dodecyl sulfate-stable oligomers in cell culture. *J. Biol. Chem.* 270, 9564–9570.
- (28) Sadrzadeh, S. M., and Bozorgmehr, J. (2004) Haptoglobin phenotypes in health and disorders. *Am. J. Clin. Pathol.* 121 (Suppl), S97–104.
- (29) Saeed, S. A., Ahmad, N., and Ahmed, S. (2007) Dual inhibition of cyclooxygenase and lipoxygenase by human haptoglobin: its polymorphism and relation to hemoglobin binding. *Biochem. Biophys. Res. Commun.* 353, 915–920.
- (30) Roheim, P. S., Carey, M., Forte, T., and Vega, G. L. (1979) Apolipoproteins in human cerebrospinal fluid. *Proc. Natl. Acad. Sci. U.S.A.* 76, 4646–4649.
- (31) Vance, J. E., and Hayashi, H. (2010) Formation and function of apolipoprotein E containing lipoproteins in the nervous system. *Biochim. Biophys. Acta, Mol. Cell Biol. Lipids* 1801, 806–818.
- (32) Holtzman, D. M., Herz, J., and Bu, G. (2012) Apolipoprotein e and apolipoprotein e receptors: normal biology and roles in Alzheimer disease. *Cold Spring Harbor Perspect. Med.* 2, a006312.
- (33) Herrup, K. (2010) Reimagining Alzheimer's disease—an age-based hypothesis. *J. Neurosci.* 30, 16755–16762.
- (34) Mawuenyega, K. G., Sigurdson, W., Ovod, V., Munsell, L., Kasten, T., Morris, J. C., Yarasheski, K. E., and Bateman, R. J. (2010) Decreased clearance of CNS beta-amyloid in Alzheimer's disease. *Science* 330, 1774.
- (35) Mattila, K. M., Pirttilä, T., Blennow, K., Wallin, A., Viitanen, M., and Frey, H. (1994) Altered blood-brain-barrier function in Alzheimer's disease? *Acta Neurol. Scand.* 89, 192–198.

(36) Cordonnier, C., and van der Flier, W. M. (2011) Brain microbleeds and Alzheimer's disease: innocent observation or key player? *Brain* 134, 335–344.

(37) Stone, J. (2008) What initiates the formation of senile plaques? The origin of Alzheimer-like dementias in capillary haemorrhages. *Med. Hypotheses* 71, 347–359.

(38) Salvatore, A., Cigliano, L., Carlucci, A., Bucci, E. M., and Abrescia, P. (2009) Haptoglobin binds apolipoprotein E and influences cholesterol esterification in the cerebrospinal fluid. *J. Neurochem.* 110, 255–263.

(39) Strittmatter, W. J., Saunders, A. M., Schmechel, D., Pericak-Vance, M., Enghild, J., Salvesen, G. S., and Roses, A. D. (1993) Apolipoprotein E: high-avidity binding to  $\beta$ -amyloid and increased frequency of type 4 allele in late-onset familial Alzheimer's disease. *Proc. Natl. Acad. Sci. U.S.A.* 90, 1977–1981.

(40) Strittmatter, W. J., Weisgraber, K. H., Huang, D. Y., Dong, L.-M., Salvesen, G. S., Pericak-Vance, M., Schmechel, D., Saunders, A. M., Goldgaber, D., and Roses, A. D. (1993) Binding of human apolipoprotein E to synthetic amyloid  $\beta$  peptide: isoform-specific effects and implications for late-onset Alzheimer disease. *Proc. Natl. Acad. Sci. U.S.A.* 90, 8098–8102.

(41) Jordán, J., Galindo, M. F., Miller, R. J., Reardon, C. A., Getz, G. S., and LaDu, M. J. (1998) Isoform-specific effect of apolipoprotein E on cell survival and beta-amyloid-induced toxicity in rat hippocampal pyramidal neuronal cultures. *J. Neurosci.* 18, 195–204.

(42) LaDu, M. J., Reardon, C., Van Eldik, L., Fagan, A. M., Bu, G., Holtzman, D., and Getz, G. S. (2000) Lipoproteins in the central nervous system. *Ann. N.Y. Acad. Sci.* 903, 167–175.

(43) Manelli, A. M., Stine, W. B., Van Eldik, L. J., and LaDu, M. J. (2004) ApoE and Abeta1–42 interactions: effects of isoform and conformation on structure and function. *J. Mol. Neurosci.* 23, 235–246.

(44) Krako, N., Magnifico, M. C., Arese, M., Meli, G., Forte, E., Lecci, A., Manca, A., Giuffrè, A., Mastronicola, D., Sarti, P., and Cattaneo, A. (2013) Characterization of mitochondrial dysfunction in the 7PA2 cell model of Alzheimer's disease. *J. Alzheimer's Dis.* 37, 747–758.

(45) Meli, G., Lecci, A., Manca, A., Krako, N., Albertini, V., Benussi, L., Ghidoni, R., and Cattaneo, A. (2014) Conformational targeting of intracellular A $\beta$  oligomers demonstrates their pathological oligomerization inside the endoplasmic reticulum. *Nat. Commun.* 5, 3867–3884.

(46) Bradford, M. M. (1976) A rapid and sensitive method for the quantitation of microgram quantities of protein utilizing the principle of protein-dye binding. *Anal. Biochem.* 72, 248–254.

(47) Cigliano, L., Spagnuolo, M. S., and Abrescia, P. (2003) Quantitative variations of the isoforms in haptoglobin 1–2 and 2–2 individual phenotypes. *Arch. Biochem. Biophys.* 416, 227–237.

(48) Stine, W. B., Dahlgren, K. N., Krafft, G. A., and LaDu, M. J. (2003) In vitro characterization of conditions for Amyloid- $\beta$  peptide oligomerization and fibrillogenesis. *J. Biol. Chem.* 278, 11612–11622.

(49) Chen, C.-H., and Albers, J. J. (1982) Characterization of proteoliposomes containing apoprotein A-I: a new substrate for the measurement of lecithin:cholesterol acyltransferase activity. *J. Lipid Res.* 23, 680–691.